

Long-term investigation of a deep-seated creeping landslide in crystalline rock. Part II. Mitigation measures and numerical modelling of deep drainage at Campo Vallemaggia

E. Eberhardt, L. Bonzanigo, and S. Loew

Abstract: For more than 200 years, the villages of Campo Vallemaggia and Cimalmotto have been slowly moving on top of a deep-seated landslide in the southern Swiss Alps. Numerous mitigation measures have been carried out during this time to stabilize the landslide but with limited to no success. Those attempts largely focussed on minimizing erosion at the toe of the landslide. More recently, the need to stabilize the slope began to intensify, as with each passing year the two villages were being pushed closer to the edge of a 100 m high erosion front at the foot of the landslide. This led to an extensive investigation and monitoring campaign to better understand the factors controlling the landslide movements, which as reported in Part I (see companion paper, this issue), pointed to high artesian pore pressures as being the primary destabilizing mechanism. Here in Part II, the arguments supporting the need for a deep drainage solution are reported, as is the history, implementation, and measured response of the Campo Vallemaggia landslide to the various mitigative measures taken. Numerical modelling results are also presented, based on hydromechanically coupled distinct-element models, to help demonstrate why deep drainage succeeded where other mitigation measures failed.

Key words: deep-seated landslide, mitigation, drainage adit, distinct-element method, coupled hydromechanical analysis.

Résumé : Depuis plus de 200 ans, les villages de Campo Vallemaggia et de Cimalmotto ont bougé lentement à la surface d'un glissement profond dans la partie sud des Alpes suisses. Plusieurs mesures de confortement ont été réalisées durant cette période pour stabiliser le glissement, mais avec peu ou pas de succès. Ces travaux se sont concentrés sur le contrôle de l'érosion au pied du glissement. Plus récemment, le besoin de stabiliser la pente est devenu critique alors que, avec chaque année qui passait, les deux villages se sont rapprochés de plus en plus près du bord d'un front d'érosion de 100 m de hauteur au pied du glissement. Ceci a conduit à une investigation étendue poussée et à une campagne de mesures pour mieux comprendre les facteurs contrôlant les mouvements du glissement qui, comme on en a fait état dans la Partie 1 de cet article, identifiaient les fortes pressions artésiennes comme étant les principaux mécanismes de déstabilisation. Ici dans la Partie 2, on fait rapport des arguments à l'appui du besoin d'une solution de drainage en profondeur, de même que de l'histoire, de la mise en place et de la réponse du glissement de Campo Vallemaggia aux diverses mesures de confortement appliquées. On présente aussi plusieurs résultats de modélisations basées sur des modèles en éléments distincts hydro-mécaniques couplés pour aider à démontrer pourquoi le drainage profond a réussi là où d'autres mesures de confortement ont échoué.

Mots-clés : glissement profond, confortement, galerie de drainage, méthode des éléments distincts, analyse hydro-mécanique couplée.

[Traduit par la Rédaction]

Introduction

The Campo Vallemaggia deep-seated creeping landslide encompasses approximately 800 million cubic metres of fractured and weathered crystalline rock. Surface and borehole investigations of the unstable mass suggest that the yield and sliding surface (actually a zone several metres

thick) reaches depths of up to 300 m (see Part I, Bonzanigo et al. 2007). Prior to the mitigation works described in this paper, geodetic measurements showed a typical movement rate of 5 cm/year, although because of several short periods of acceleration, an average rate of 30 cm/year could be calculated over the past 100 years. These slope displacements continuously caused damage to roads and buildings located

Received 31 March 2006. Accepted 14 April 2007. Published on the NRC Research Press Web site at cgj.nrc.ca on 27 November 2007.

E. Eberhardt,^{1,2} L. Bonzanigo,³ and S. Loew. Engineering Geology, Swiss Federal Institute of Technology (ETH Zurich), Hoenggerberg, CH-8093 Zurich, Switzerland.

¹Corresponding author (e-mail: erik@eos.ubc.ca).

²Present address: Geological Engineering, Department of Earth and Ocean Sciences, 6339 Stores Rd, The University of British Columbia, Vancouver, BC V6T 1Z4, Canada.

³Present address: geolog.ch Ltd, Geologi Consulente, Box 1152, CH-6501 Bellinzona, Switzerland.

on the slide mass. Of even greater concern, however, was the precarious position of two villages located on the lower part of the slide body (Campo Vallemaggia and Cimalmotto), which with each passing year, moved closer to the edge of a steep 100 m high erosion front cut by the Rovana River at the slide's toe (Fig. 1).

An effective mitigation plan was therefore deemed necessary to stabilize the slope, and emergency plans for the evacuation of the people living in Campo Vallemaggia were prepared in case the situation became critical. Two different sets of stabilization measures were proposed, however, as expert opinions differed as to the underlying processes driving the instability. One opinion saw the continuous heavy erosion of the landslide's toe by the Rovana River as being the primary driving factor and called for the partial diversion of the river to stabilize the landslide. The second opinion concluded that hydrogeological controls were the underlying cause and that a deep drainage option would be more effective.

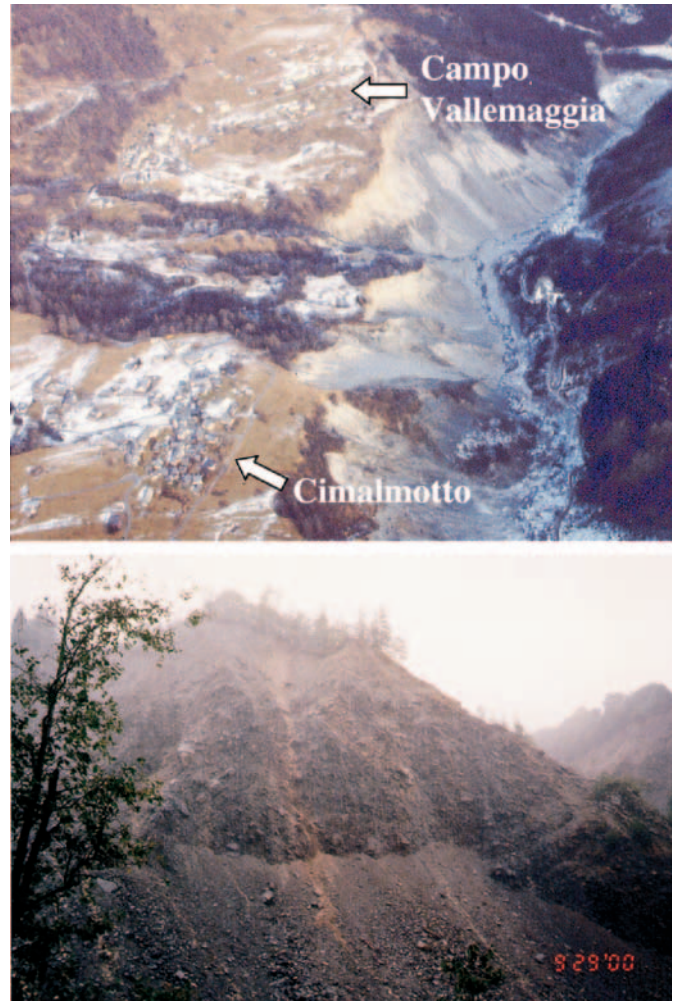
In fact, these conflicting opinions were historical in nature. Numerous attempts to control erosion at the toe of the landslide had been carried out in the past, beginning in 1888. During his investigation of Campo Vallemaggia in 1897, Albert Heim cited the presence of several springs with flow rates of 1 to 5 m³/min as being significant (Heim 1897, 1932). Although his understanding of the exact role pore pressures play in destabilizing a slope was limited, as it preceded Terzaghi's effective stress concept (e.g., Terzaghi 1950), Heim stressed the need to divert groundwater from the landslide to stabilize it.

In 1993, steps were taken to construct both a river diversion tunnel and a deep drainage adit. The supporting arguments that led to the financing of the deep drainage mitigation solution were based on a detailed mapping and monitoring investigation performed from 1983 to 1991, as reported in Part I (Bonzanigo et al. 2007). Here in Part II, the history of mitigation works at Campo Vallemaggia is reviewed together with that of the 1993–1995 drainage adit construction. Pore pressure and displacement measurements taken before and after completion of the drainage works are presented, together with a series of hydromechanically coupled distinct-element models that were used to provide further insights into the means by which deep drainage helped stabilize the landslide.

History of mitigation schemes employed at Campo Vallemaggia

The first attempts to stabilize the Campo Vallemaggia landslide were carried out in 1888, following earlier logging activity and an 1867 rockfall from the opposite side of the valley that combined to push the river towards the toe of the landslide, significantly increasing the downcutting action at the landslide's toe to form a 150 m high scarp (Fig. 1). The overwhelming appearance of the erosion front left the impression on most experts and decision makers that erosion and loss of toe support was the instigating force driving the landslide movements. As such, the stabilization works carried out focussed on erosion control through the construction of a series of boulder weirs and check dams in front of the slide mass (Fig. 2). The insufficiency of these measures,

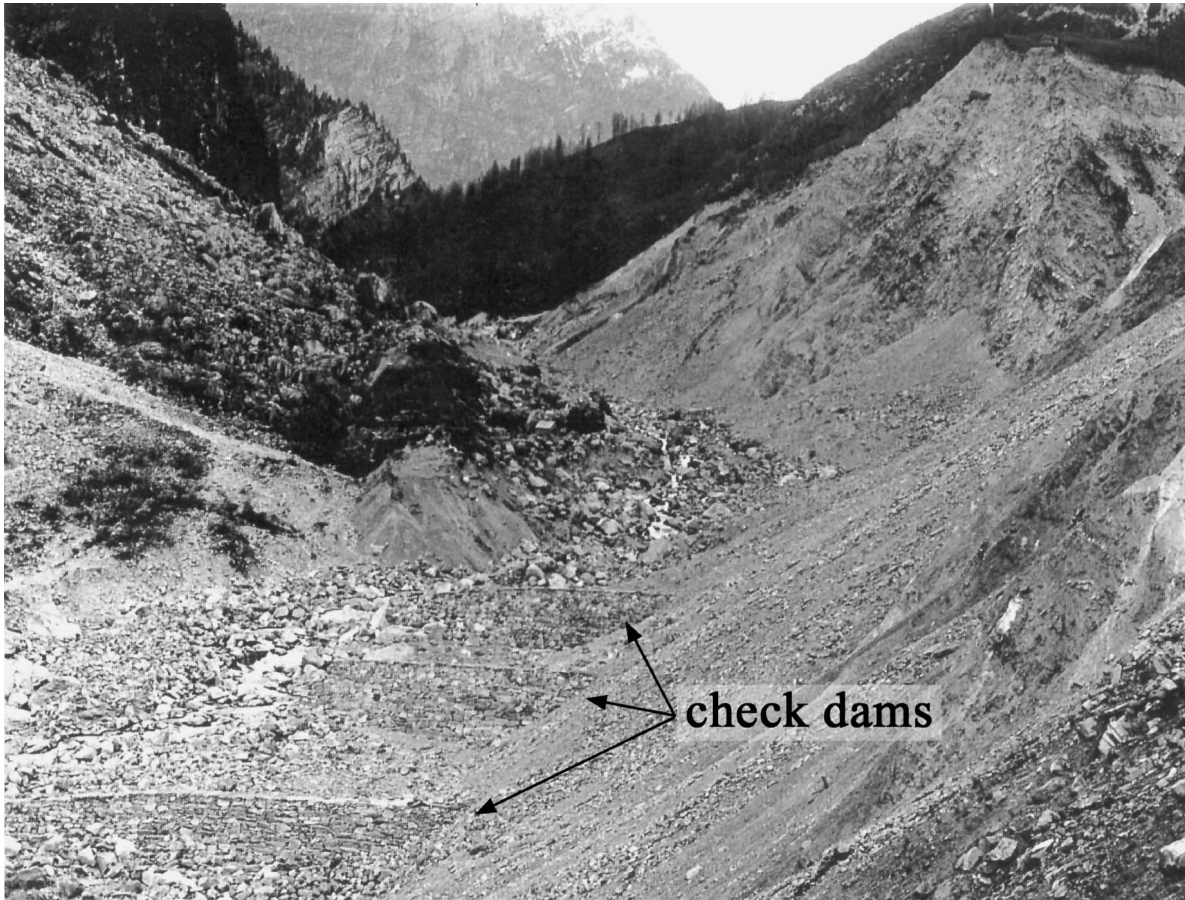
Fig. 1. Views of the erosion scarp formed at the toe of the Campo Vallemaggia landslide. Note in upper photo the location of the villages of Cimalmotto and Campo Vallemaggia near the edge of the erosion front. The vegetated area in the middle left of this photo marks the approximate location of the lateral fault that divides the landslide into the Campo and Cimalmotto blocks (see Fig. 4). The latitude and longitude of the two villages are: Cimalmotto, 46°17'01"N, 8°29'23"E; Campo Vallemaggia, 46°17'22"N, 8°29'41"E. The view in the bottom photo is looking northwest towards the toe of the Campo block.



however, was quickly exposed the following year when most of the check dams were completely destroyed and swept away by flooding of the river.

In the early 1930s, mitigative efforts turned to the intensive planting of alder trees and brush. During this period, measures were also taken to control surface runoff through the construction of diversion drains. From 1940 to 1945, these works were modified and improved to include the addition of wood linings to the drainage ditches. These measures appeared to help reduce damage to surface structures, but had no effect on the movements of the slide body as a whole. Over time, the differential movements of the slide body slowly destroyed this system of drains despite continuous maintenance by the local population. This led to a major effort to rebuild the system between 1993 and 1996, restor-

Fig. 2. A photo taken in 1890 of the transversal check dams built to control the erosion along the toe of the Campo Vallemaggia landslide. The check dams were subsequently washed away later the same year during flooding of the river. The toe of the landslide appears along the right half of the photo.



ing the diversion drains to include cemented stone and renewed wood linings.

In 1986, efforts again refocused on trying to stabilize the landslide through erosion control measures. A reinforced concrete weir with a holding capacity of approximately 800 000 m³ was constructed at the foot of the landslide (where the bedrock outcrops) to hold back eroded material. Soon after, following a period of intense precipitation and erosion in 1987, the concrete weir and dam structure had completely filled.

During this time, slope movements began to accelerate reaching velocities of 1 m/year. By the 1990s the situation at Campo Vallemaggia was growing more perilous, with little consensus being reached as to the next steps required to stabilize the slope. Results from the detailed geological, hydrogeological, and geotechnical investigations, then recently completed, leaned heavily towards a deep drainage solution (see Part I, Bonzanigo et al. 2007). Yet despite a long history of failed attempts, many still favoured a solution concentrating on erosion control. The often acrimonious direction these differing opinions took eventually led to a decision to implement both options. The first involved the construction of a 7 m diameter diversion tunnel, started in 1993 and completed in 1996, through the valley wall opposite the Campo Vallemaggia landslide to redirect the river away from the erosion front and slide toe (Fig. 3). In parallel, a deep drain-

age adit was also constructed (1993–1995) below the unstable slide mass from which drainage boreholes were drilled upwards into the base of the landslide body (Fig. 4).

Mitigation by deep drainage at Campo Vallemaggia

The construction of a drainage tunnel within or under the slide mass had first been proposed by Albert Heim in the late 1890s during his investigation of the Campo Vallemaggia landslide, but was met with much political resistance (Heim 1897). Between 1964 and 1971, the call for a deep drainage solution was again forwarded and again did not receive much support (Lichtenhahn 1971). Finally in 1991, backed by detailed mapping and instrumentation data (Bonzanigo 1999) and an expert opinion by Dr. Giovanni Lombardi (not published), plans for the drainage adit received the necessary authorization for a design to be developed. Construction then began in October 1993 and was completed in July 1995.

Construction of the drainage adit

The design of the drainage adit (by Lombardi Ltd. and L. Bonzanigo; Lombardi 1996) called for the construction of a tunnel with a 3.6 m span (11 m² in cross-sectional area) and 1810 m length. The positioning of the adit was planned based on data collected from the investigation boreholes and

Fig. 3. Photos of diversion tunnel constructed to divert the Rovana River away from the toe of the Campo Vallemaggia landslide (see Fig. 4 for location).



seismic survey (see Part I for details, Bonzanigo et al. 2007). The excavation entered the subsurface from outside the eastern boundary of the slide mass through 100 m of overburden (Fig. 4) and continued on through the undisturbed rock below the landslide (Fig. 5). The portal was located at elevation 1075 m a.s.l. and was excavated by drill and blast with an upward 2% grade to facilitate drainage of the adit. Initially, 120 drainage boreholes were planned but this number was later reduced (and the lengths extended) after it was recognised that there was no well-defined, discrete, sliding surface, but rather a transition zone between sound rock and the sliding mass. Thirty boreholes, varying in length between 25 and 70 m, were then drilled into the transition zone through which the basal shear surface passed (Fig. 5).

During construction of the drainage adit, numerous hypotheses regarding the subsurface geology and hydrogeology were confirmed. Tunnel mapping confirmed the presence of numerous sub-vertical fault zones at depth (Fig. 6a), together with sets of secondary faults dipping at 50° . The fault zones were initially hypothesized as being structures along which strong vertical flow paths had developed leading to artesian conditions at the base of the sliding surface (see Part I, Bonzanigo et al. 2007). Direct observations during tunnel excavation revealed that the fractured rock mass bounding the central gouge zone was highly permeable relative to that of the gouge and undamaged host rock (Fig. 6b–6c). Thus in the proximity of these subvertical fault zones, flow would be restricted horizontally due to the low permeability gouge but enhanced vertically along the associated damage zones. This was likewise reflected in the hydrogeochemical signatures of water samples collected from springs at surface and within the drainage adit (Bonzanigo 1999).

During the first 1000 m of adit construction, driven in a northwest direction, the tunnelling conditions were virtually dry and only small water inflows were periodically encountered. The design then called for a bend in the tunnel axis from which it would proceed in a southwest direction (Fig. 4). From this redirection point, a 100 m long investigation borehole was drilled ahead of the tunnel, which intersected a water bearing fault zone showing 32 bar (1 bar = 100 kPa) of static pressure (an equivalent piezometric head of 1420 m a.s.l.). This was the same order of magnitude measured by a piezometer pressure device installed at 178 m depth in borehole CVM6 (surface borehole collar at 1333 m a.s.l.), where initial artesian overpressures of 23 bar were measured (see Part I for the details regarding the pre-drainage borehole measurements; Bonzanigo et al. 2007).

Once the adit was completed, the total outflow at the portal was measured to be 9 L/s, of which 5 L/s were produced from the last 20 m of the adit. Within this zone, after having passed through a tectonized zone, the massive brittle gneisses were more densely fractured and noticeably more permeable than the cataclastic faults previously encountered. In 1995, construction then proceeded with the drilling of drainage boreholes upwards into the base of the slide mass from different locations along the last 1000 m of the adit. One of these, with a length of 48 m, produced a peak flow of 30 L/s. Following the completion of 35 of the 120 originally planned boreholes, the total discharge at the adit portal was measured to be 50 L/s (at the end of 1995). By 1998, the drainage flow from the adit system was 30 L/s. The location of these boreholes along the drainage adit and the respective outflows are shown in Fig. 7.

Measured response of the slide mass to deep drainage

The measured pore pressure response within borehole CVM6 to these drainage boreholes was surprisingly immediate – an approximate drop in head of 150 m was achieved (Fig. 8). As described in Part I (Bonzanigo et al. 2007), CVM6 was located within the Campo block, the more unstable of the two blocks forming the landslide body. Figure 9 compares the before and after pore pressure distributions within the Campo block based on surface piezometer readings and those made from within the drainage adit. As a consequence of deep drainage, the upward flow of groundwater

Fig. 4. Locations of the Rovana River diversion tunnel and Campo Vallemaggia landslide drainage adit. The photos shown in Figs. 1 and 2 are looking northwest towards the shaded area marked below as the erosion front.

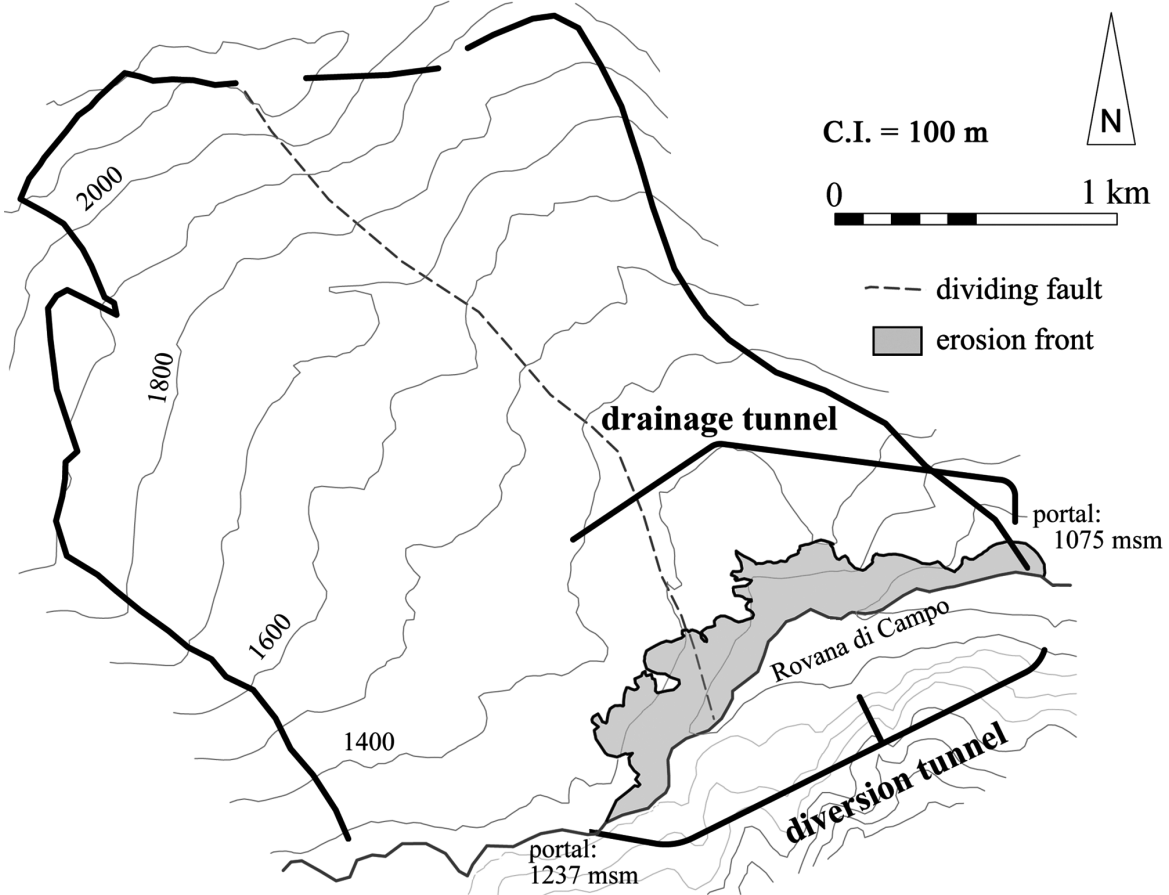
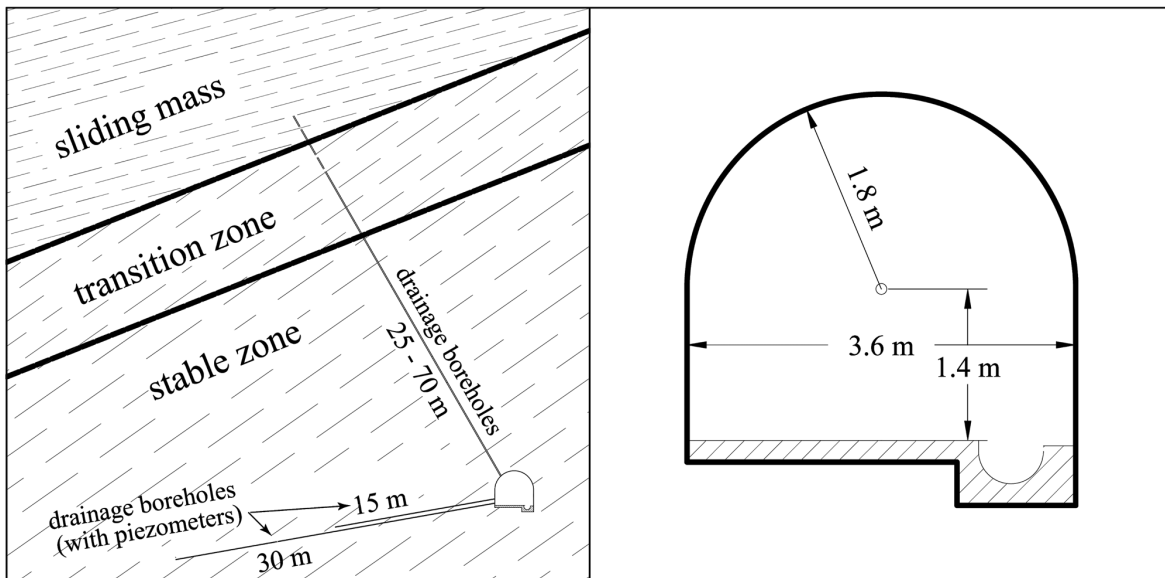


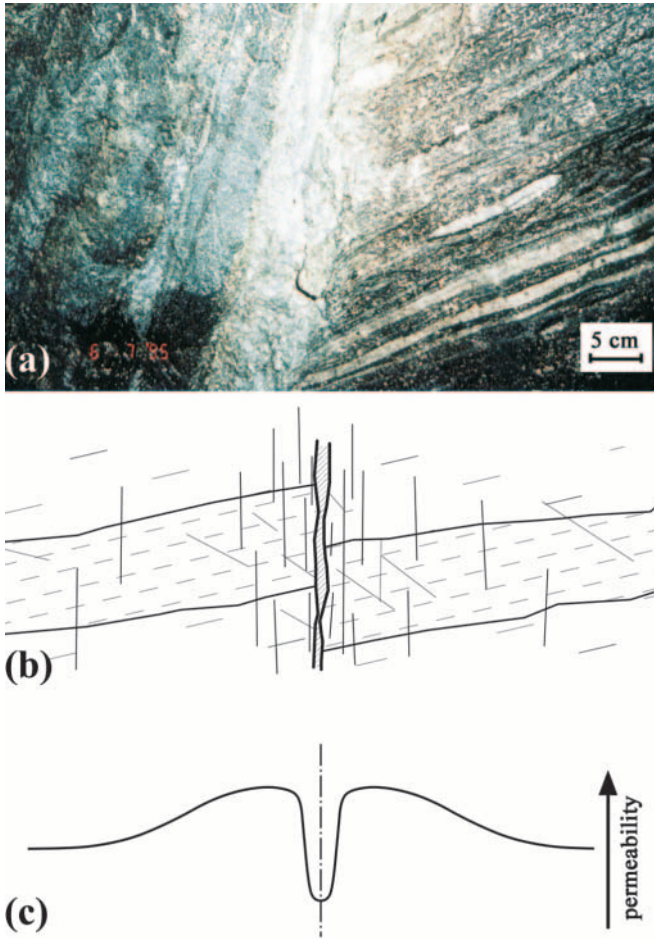
Fig. 5. Schematic illustration of the drainage adit design with perforated cased drainage boreholes (left) and adit profile (right).



through the unstable transition zone beneath the foot of the landslide (Fig. 9a) is redirected towards the adit (Fig. 9b). In borehole CVM4, located in the neighbouring Cimalmotto block, the measured response was detectable but less noteworthy (Fig. 10).

The response of the landslide was likewise immediate (Fig. 11). The reversal of the pore pressure gradient within the landslide transition zone was seen to quickly stabilize the Campo block through the subsequent increase in effective stress and resisting forces along its basal shear surface. Again,

Fig. 6. Photo (a) and schematic representation (b) of a typical sub-vertical fault zone intersected below the sliding surface during excavation of the drainage adit. (c) Illustration of permeability anisotropy observed across the brittle fault structure.



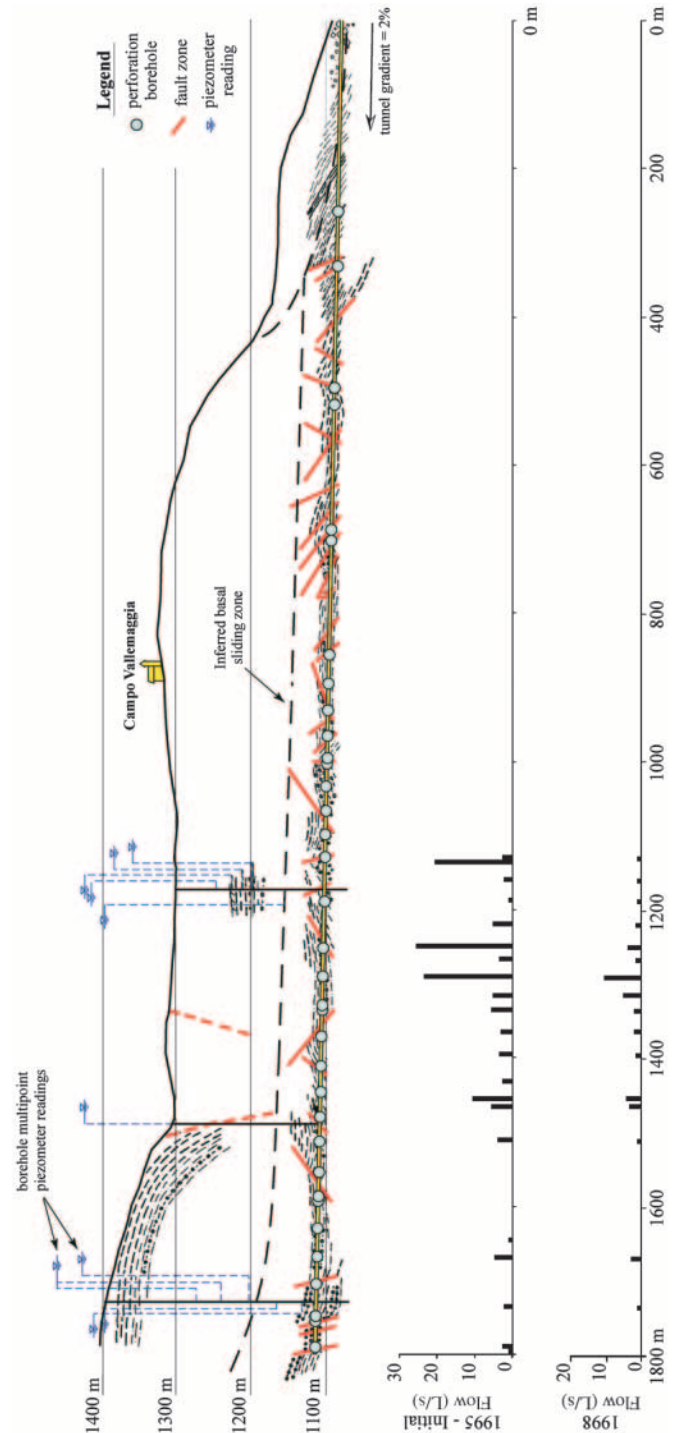
it was quite interesting to note the quickness of this process despite the overall low permeability of the crystalline rock and immense volume of material involved in the instability.

Geodetically measured slope movements were seen to decrease significantly across the entire slide mass, and in some cases, upslope displacements were recorded relating to the development of a subsidence cone. Surface geodetic measurements revealed that up to 40 cm of vertical consolidation subsidence occurred directly over the drainage adit (Fig. 12). Given the kinematic constraints imposed on the Cimalmotto block by the Campo block (described in Part I, Bonzanigo et al. 2007), the stabilization of the Campo block had a similar stabilizing effect on the Cimalmotto block.

Distinct-element modelling of the stabilization works

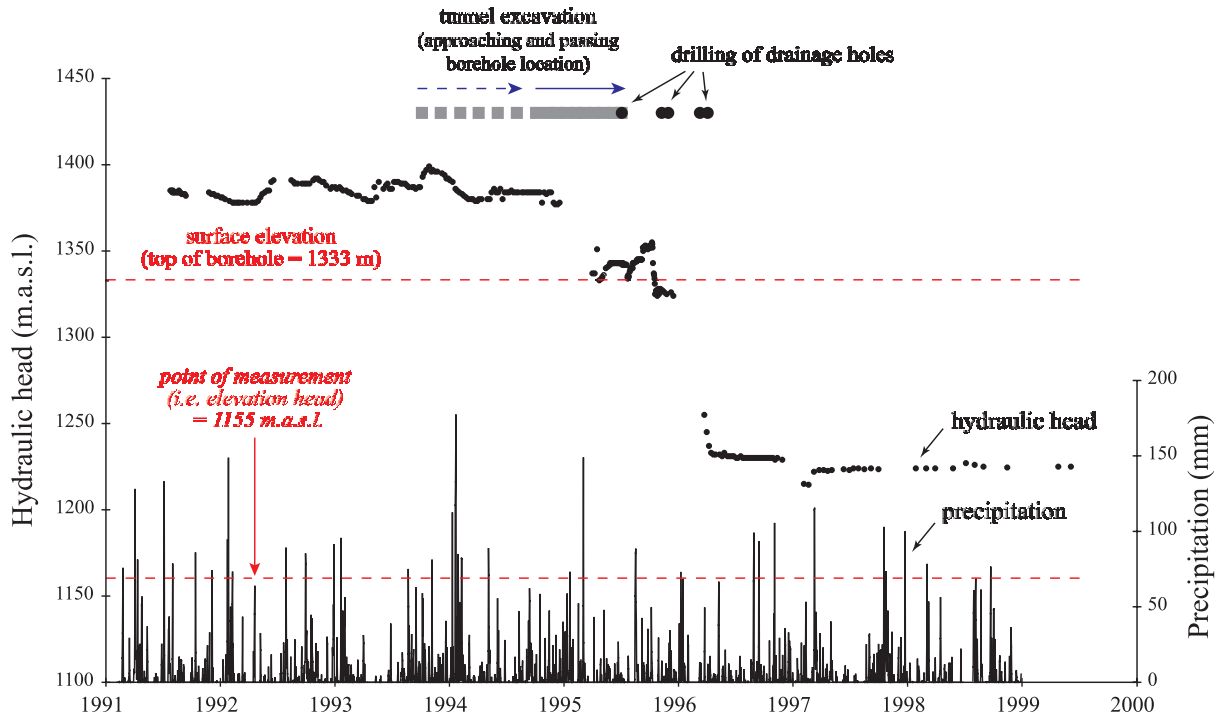
Despite the apparent success of the deep drainage mitigation solution, its effectiveness was soon called into question. This was largely based on two arguments. The first was that both the drainage adit and the river diversion (i.e., toe erosion protection) solutions were implemented simultaneously, and thus proponents of either could claim success in stabilizing the landslide. The second centred on the perceived low

Fig. 7. Drainage adit profile showing brittle fault zones intersected and locations of drainage boreholes, with respective initial (i.e., 1995) and 1998 measured outflows. See Fig. 4 for drainage adit location in plan view.



outflow rates from the drainage adit (<30 L/s) given the volume of the slide mass supposedly drained. This became a critical issue, even though in either event the landslide had been stabilized, because over the long term, the drainage adit and drainage boreholes would require regular inspection, maintenance, and reconditioning to ensure their continued effectiveness. The lack of further evidence dem-

Fig. 8. Measured pore pressures in borehole CVM6 (Campo block) before, during, and after construction of the drainage adit and drilling of the perforation boreholes. Pore pressures are expressed in terms of hydraulic head (i.e., elevation of the water column in the piezometer).



onstrating the effectiveness of the deep drainage solution raised the possibility that the proper resources would not be budgeted for continued monitoring, and the drainage adit system may fall into neglect leading to the reactivation of the landslide movements.

Numerical modelling was therefore used to test the two mitigation solutions implemented and to strengthen the argument as to why the drainage adit system was effective and should be maintained, despite the low outflow rates.

Model setup

A coupled discrete hydromechanical approach was adopted using the commercial distinct-element program UDEC (Itasca 2004). Geological field data collected through the mapping campaign (see Part I, Bonzanigo et al. 2007) and pore pressure and displacement measurements obtained through the instrumentation network were used to constrain the models. Models were created using a representative 2-D section through the Campo block of the slide body (Fig. 13; see also Figs. 3 and 4 in Part I; Bonzanigo et al. 2007). This cross-section was chosen as it best represented the primary instability mode, namely the translational sliding of the Campo block as opposed to the creep-like deformations of the Cimalmotto block, which as previously noted is kinematically constrained by the Campo block.

The discontinuity network geometry was generated to portray the strong horizontal anisotropy within the slide body and the vertical anisotropy below it. The upper slopes were modelled as being stronger than the lower half (Fig. 13b) to reflect observed differences in the rock mass characteristics between the upper head and lower foot of the slide. Material properties were based on field observations and back calculation, and in situ stresses were set assuming a horizontal to

vertical stress ratio, K (i.e., σ_H/σ_V), of 0.5. Table 1 shows the properties used for the modelling; the undisturbed rock forming the base of the slope is modelled as elastic, and the landslide material is modelled as elastoplastic.

Figure 13 shows the model geometries used to test the stabilizing influence of the two mitigation scenarios in question. The first (Fig. 13a) reflects the stabilizing effects of erosion control at the toe of the slope. In this model, 100 years of erosion (i.e., since Heim’s initial investigation) was undone and the material absent from the present-day toe scarp was put back in place to buttress the toe. The second geometry (Fig. 13b) represents the deep drainage conditions, and includes the present-day erosion scarp, the drainage adit below the slide mass, and four drainage boreholes extending up into its base (within the plane of the 2-D cross-section).

Model hydromechanical constraints

Fracture permeability

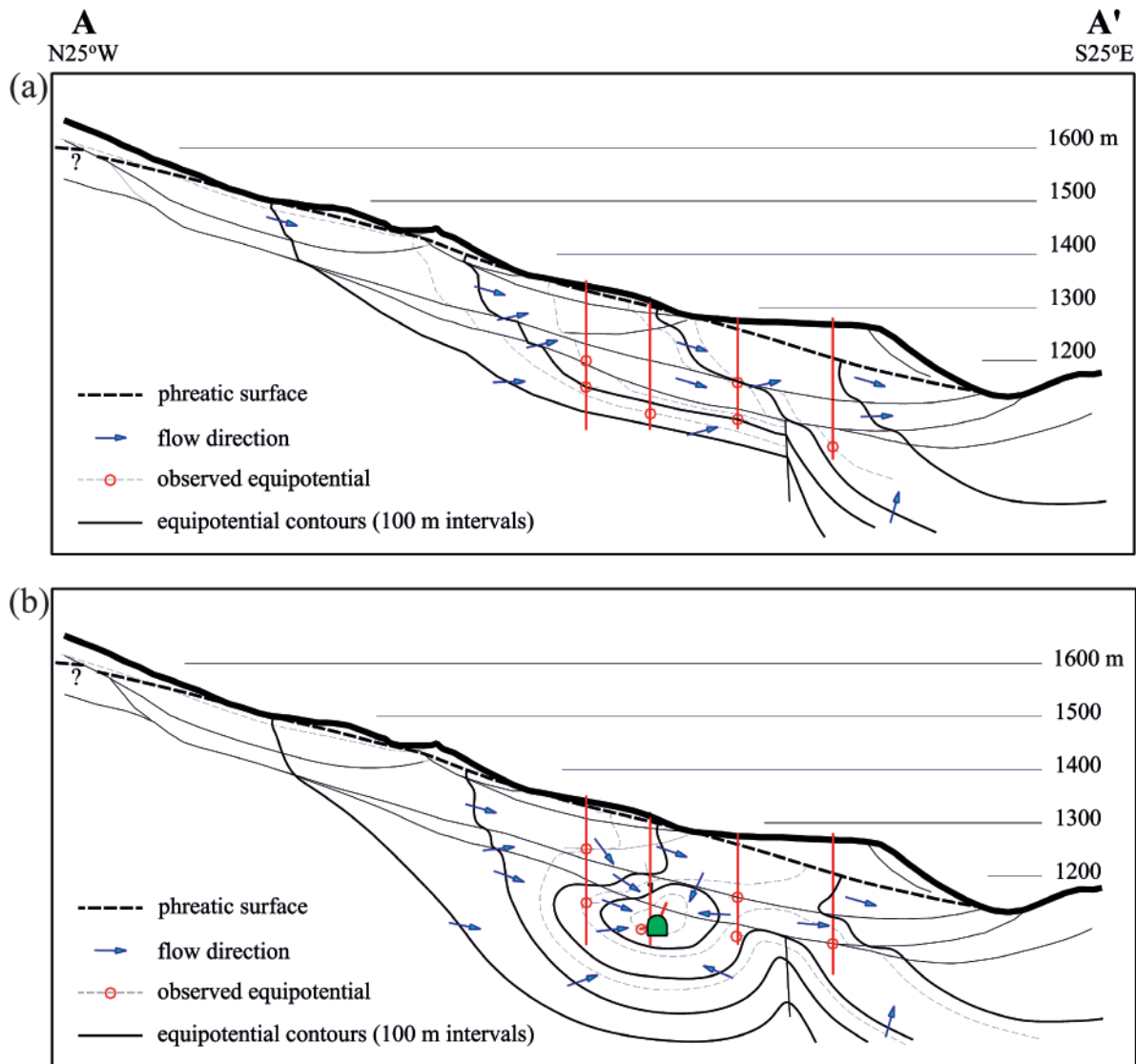
Permeability and fluid flow in the UDEC formulation are controlled by the input for fracture aperture based on the cubic law

$$[1] \quad K_{RM} = \frac{a^3 \lambda g \rho_w}{12 \mu_w}$$

$$[2] \quad q = \frac{a^3}{12 \mu_w} \frac{dp}{dl}$$

where K_{RM} is the apparent rock mass permeability (m/s); a is the contact hydraulic aperture (m); λ is the normal fracture frequency (1/m); g is the acceleration due to gravity (m/s²); ρ_w is the density of water (kg/m³); μ_w is the dynamic

Fig. 9. Semiquantitative 2-D hydrodynamic flow model of the lower Campo block: (a) before and (b) after opening of the drainage adit, showing piezometric observations, equipotential contours, and groundwater flow vectors. See Part I, Fig. 3 (Bonzanigo et al. 2007) for location of cross-section A–A'.



viscosity of water (i.e., 1×10^{-3} Pa·s); q is the unit flow rate ($\text{m}^3/\text{s}\cdot\text{m}$); and dp/dl is the hydraulic gradient for a fracture of unit width (Pa/m) (see Priest 1993).

Below the sliding mass, as observed during construction of the drainage adit, the water conducting fault zones were mapped as being predominantly subvertical (see Figs. 6 and 7). Within the landslide body, surface observations indicated that the fracture permeability was much more complex given the disturbed state of the rock. Still, the rapid development of a subsidence trough above the drainage adit (Fig. 12) suggested that at least part of the slide mass (i.e., that surrounding the fracture network perforated by the drainage boreholes) drained relatively quickly.

These consolidation measurements (i.e., vertical settlements as a function of time), provided a means to estimate the permeability of the slide mass based on Terzaghi and Peck's (1967) equations for consolidation of an open homogeneous layer. Although the form of this solution limited the

treatment of the controlling fractures to that of an equivalent continuum (i.e., the fracture network is treated implicitly), the low sensitivity of the models to this input parameter only required a general approximation. Calculations also assumed that the slide body was made up of alternating horizontal layers of varying stiffness, as observed during field and borehole investigations. In other words, the consolidation modulus (the inverse of Terzaghi and Peck's coefficient of volume compressibility) was varied as a function of the subsurface geology.

The results from this analysis are provided in Fig. 14. In it, settlement curves for several different rock mass permeabilities are plotted as a function of time. Measured values obtained from surface geodetic measurements are then superimposed on the plot (shown as open circles in Fig. 14). Here it can be seen that the measured points most closely match the curve for a permeability value of 7×10^{-6} m/s. Using eq. [1], and assuming a normal fracture frequency of 0.1, to

Fig. 10. Measured pore pressures in borehole CVM4 (Cimalmotto block) before, during, and after construction of the drainage adit and drilling of the perforation boreholes. Pore pressures are expressed in terms of hydraulic head (i.e., elevation of the water column in the piezometer).

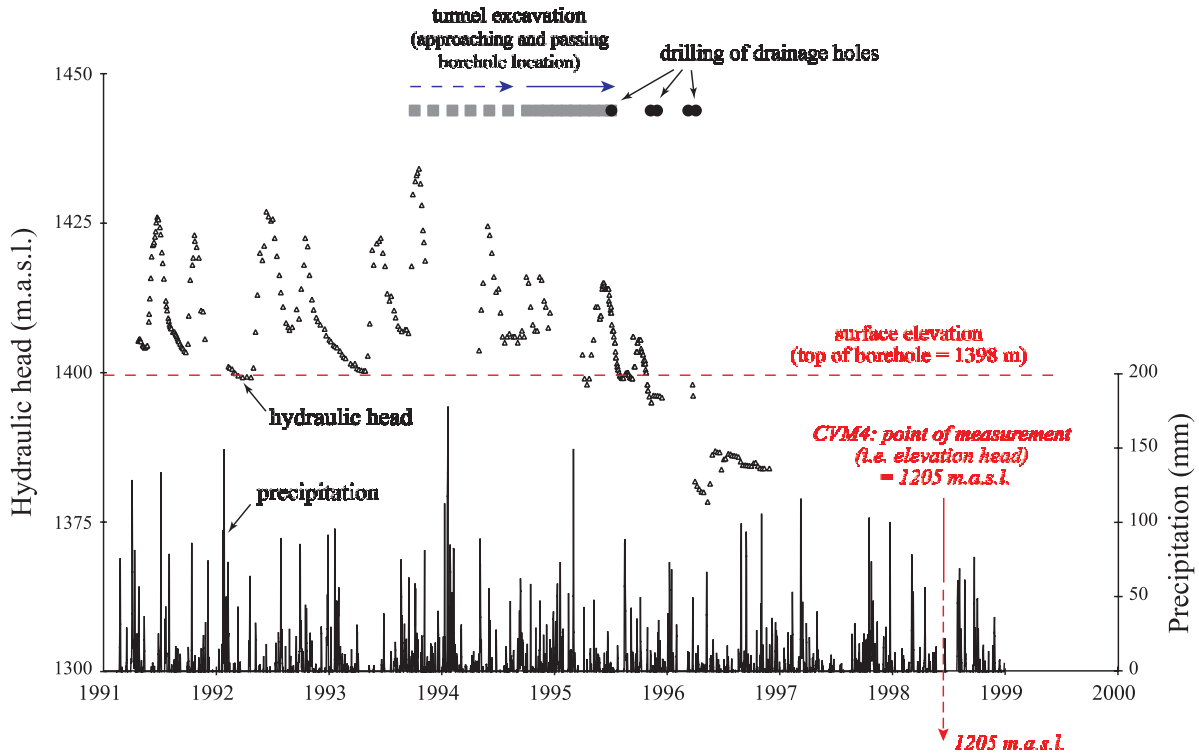
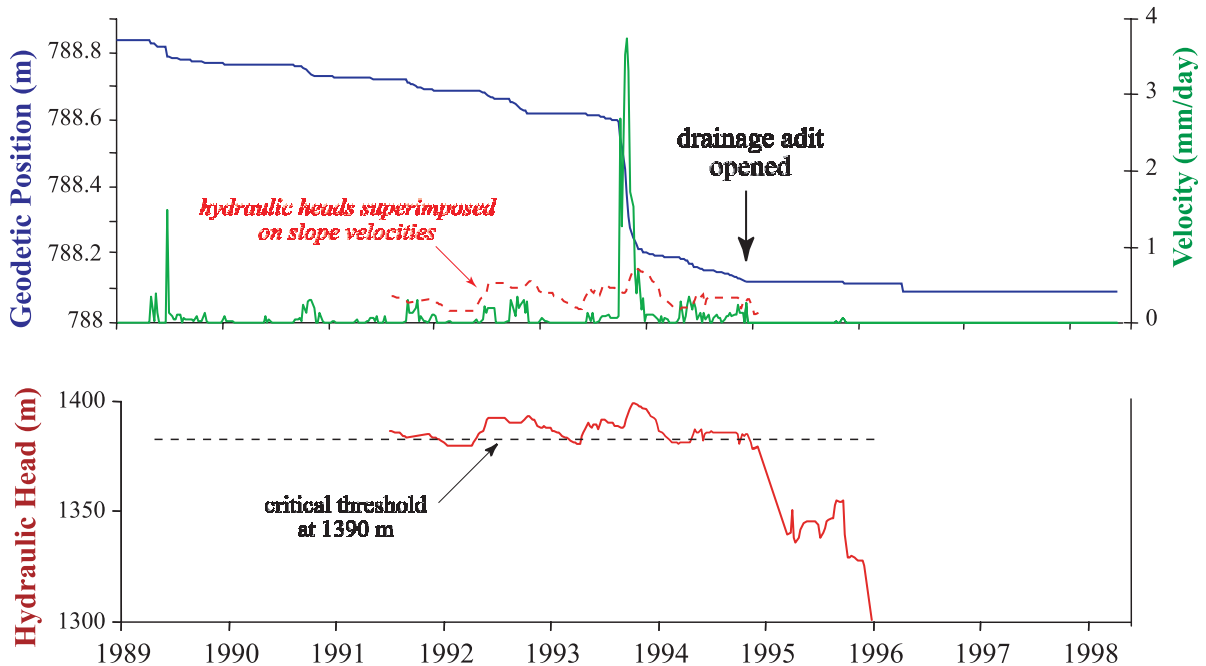


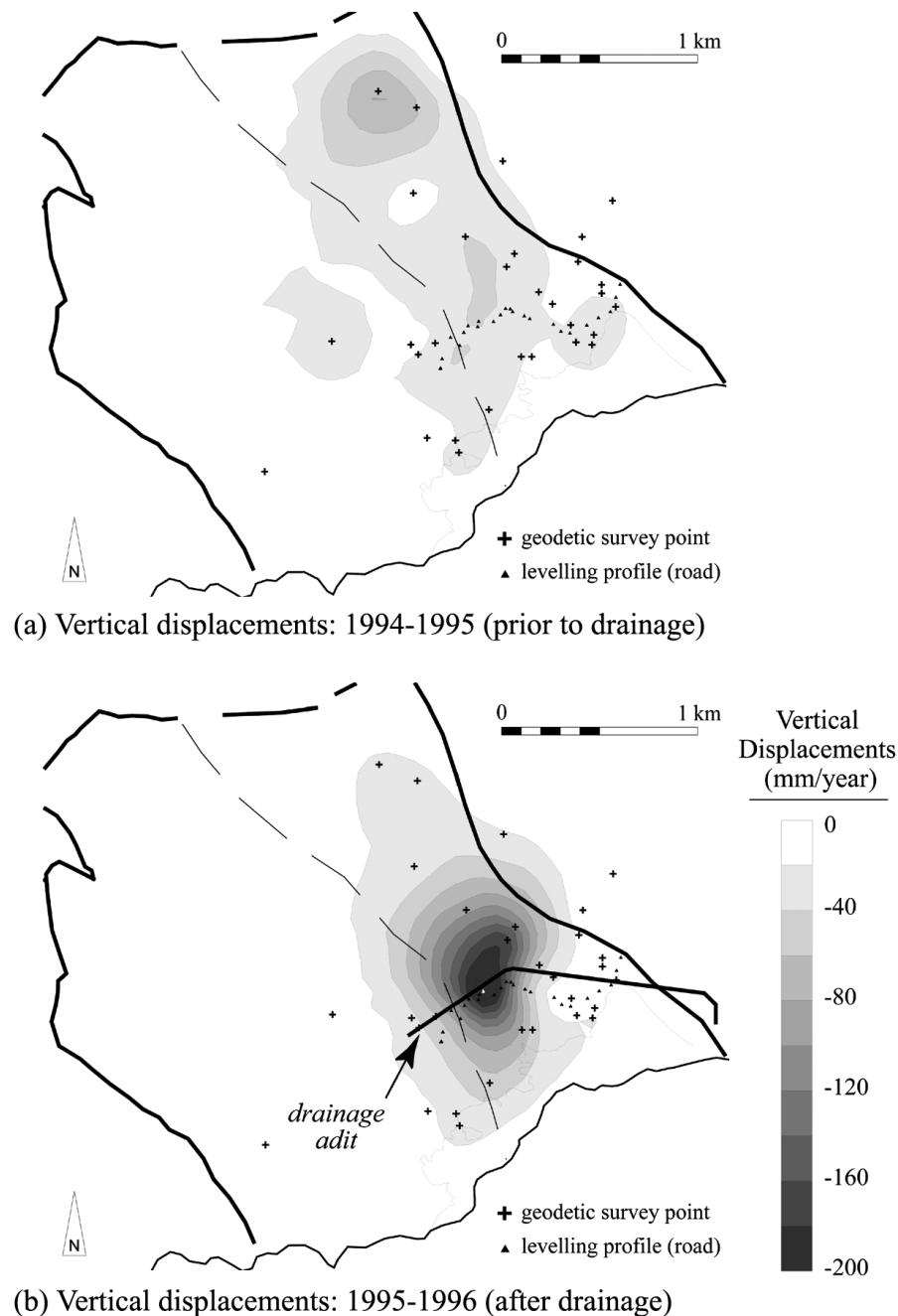
Fig. 11. Correlation between downslope velocities of the Campo block and pore pressures measured in borehole CVM6 before and after deep drainage. Slide velocities were measured using an automated geodetic station; pore pressures are expressed as the hydraulic head (i.e., elevation of the water column in the piezometer). See Part I (Bonzanigo et al. 2007) for discussion of the predrainage measurements and critical pore pressure threshold.



account for both small-scale and large-scale fractures within the slide mass, a residual fracture aperture of 0.5 mm was calculated. This value was assumed to be two times higher under zero normal stress. Furthermore, given the lower per-

meability of the slide mass relative to the undisturbed rock below the slide mass, hydraulic aperture values for the undisturbed zone were assumed to be two times higher than those within the slide mass (Table 1). This relationship was

Fig. 12. Measured differential vertical displacements: (a) before and (b) after deep drainage below the Campo block. Note the development of a subsidence trough above the drainage adit subsequent to its excavation.



justified based on observations and measurements of the undisturbed subvertical fractures made from within the drainage adit.

Pore pressure distribution

Information regarding the distribution of pore pressures in the lower parts of the landslide was somewhat better constrained than those in upper sections of the slope, due to the presence of boreholes equipped with piezometers. Pore pressures were introduced to the model using heads that correlated to in situ piezometer measurements and surface observations (Fig. 15). The assumption of a “water table” in

fractured crystalline rock slopes is tenuous at best and can be an area of considerable model uncertainty (Stead et al. 2006), especially given the degree of heterogeneity involved on the scale of a landslide as large as Campo Vallemaggia.

Still, a relatively good fit was achieved between the initial pore pressure distribution derived for the model runs and those measured in situ. Figure 16 shows the modelled pore pressure values coinciding with the location of borehole CVM6, and those measured in situ within the borehole. Both represent the long-term steady-state conditions prior to deep drainage. The variation in these values with depth, fitted with linear trend lines, can be compared with the trend

Fig. 13. UDEC model geometry of the Campo Vallemaggia slide, including: (a) slope toe without erosion (i.e., with erosion protection); (b) drainage adit and perforation boreholes. See Part I, Fig. 3 (Bonzanigo et al. 2007) for location of cross-section (i.e., A–A’).

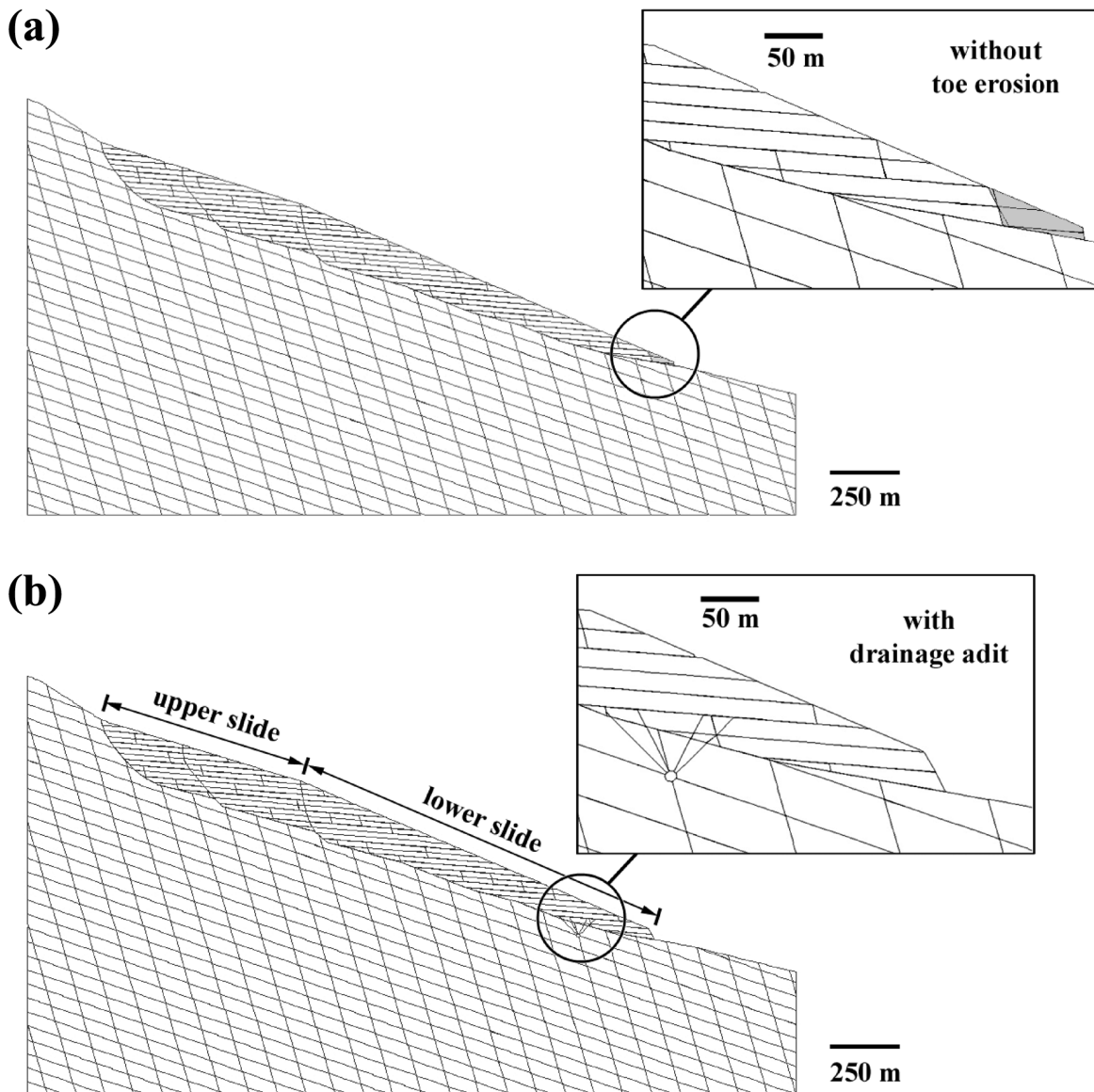


Table 1. Material properties used in UDEC simulations.

	Undisturbed rock	Upper slide body	Lower slide body
Density, ρ (kg/m ³)	2400	2300	2250
Young's modulus, E (GPa)	30	20	5
Poisson's ratio, ν	0.25	0.3	0.35
Intact cohesion, c_i (MPa)	n/a (elastic)	1	0.2
Internal friction angle, ϕ_i (°)	n/a (elastic)	45	30
Tensile strength, T_o (MPa)	n/a (elastic)	0.5	0.1
Joint friction angle, ϕ_j (°)	45	40	35
Joint cohesion, c_j (MPa)	0	0	0
Zero joint aperture, a_{zero} (mm) ^a	2	1	1
Residual joint aperture, a_{res} (mm) ^b	1	0.5	0.5

^aAperture under zero normal stress.

^bResidual aperture for high stress.

line marking hydrostatic conditions. This comparison demonstrates both the closeness in fit between modelled and in situ pore pressure distributions, and the degree of overpressure contributing to the artesian conditions at depth near the sliding surface.

Modelling results

Back calculation of slide surface strength properties

After the pore pressures in the model were initiated to correspond to those measured in situ, the frictional strength along the modelled basal shear surface was varied to back calculate its limit equilibrium state. Through this exercise, it was found that the modelled Campo block was stable for a friction angle of 34° (imposed along the sliding surface). An unstable slope resulted in the model runs for friction angles of 32° and lower. This value compares well to the 31° back-calculated using a force–balance limit equilibrium calcula-

Fig. 14. Estimates of rock mass permeability based on Terzaghi and Peck’s (1967) equations for consolidation of an open homogeneous layer. Calculations assume that the consolidation modulus varies as a function of the subsurface geology, as determined from field and borehole investigations. Measured vertical consolidation values based on surface geodetics are superimposed on the plot as open circles.

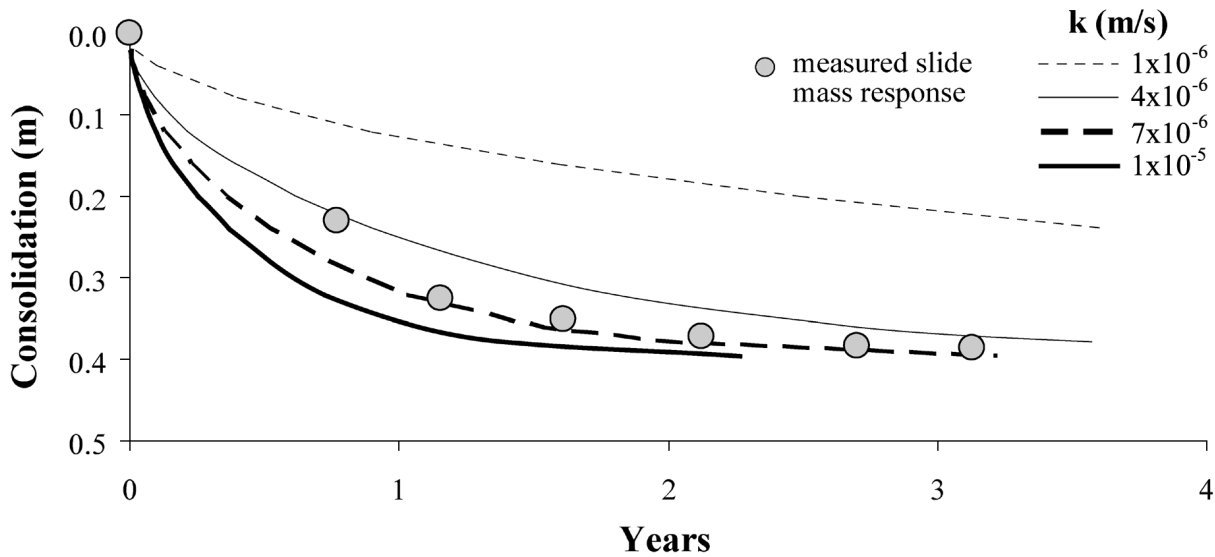
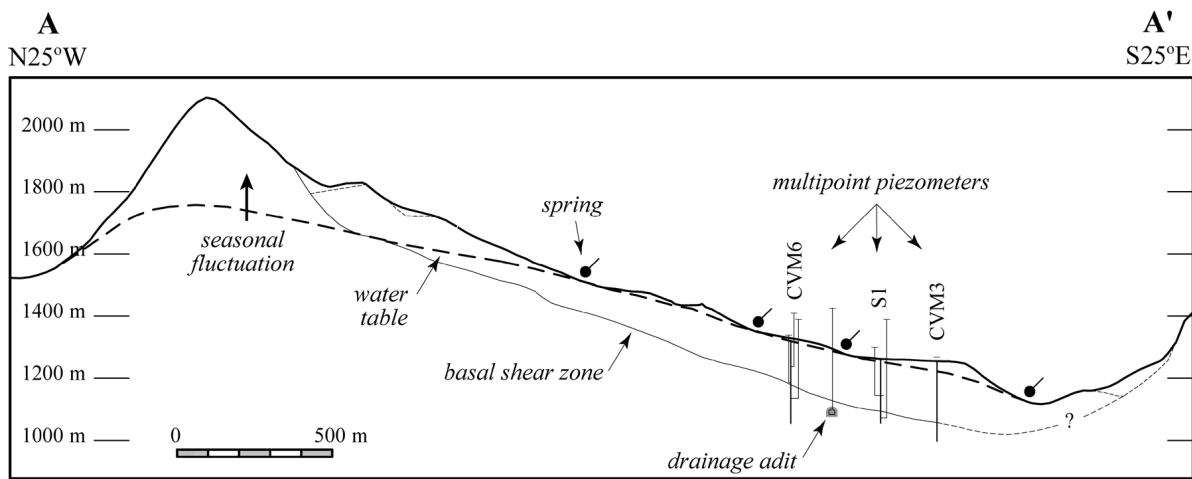


Fig. 15. Hydrogeological model used to constrain the coupled hydromechanical distinct-element models. The water table is estimated based on borehole measurements of artesian pressures and observations of surface springs. See Part I, Fig. 3 (Bonzanigo et al. 2007) for location of cross-section A–A’.



tion (presented in Part I, Bonzanigo et al. 2007). Consequently, a friction angle of 30° was assigned along the entire length of the shear-sliding surface. This value was chosen as being more conservative for modelling purposes (i.e., creating a more unstable slope condition).

Modelled effects of stabilization through erosion protection

Based on the model configuration shown in Fig. 13a, several runs were performed to test the influence of erosion protection on stabilizing the landslide. As reported in Part I (Bonzanigo et al. 2007), 11.4 million cubic metres of eroded material was estimated over the period 1888–1994, which represents just over 1% of the 800 million cubic metres approximated for the total volume of the unstable mass. In the 2-D section used to construct the UDEC model, a cross-sectional area of 280 000 m² was used to represent the un-

stable mass. Of this, the cross-sectional area of the volume eroded up to the present day scarp is 3000 m² (shaded grey in Fig. 13a), or approximately 1%.

Results from these model runs are provided in Fig. 17, where the change in stability state is depicted in terms of horizontal slope displacements. Comparisons between models where erosion of the toe has been prevented (for the past 100 years) to those that include the eroded toe scarp (without drainage) show only a slightly improved situation in terms of stability. In fact, further analysis shows that the erosion protection model requires a 10-fold (10×) increase in mass (or volume) of the material at the landslide’s toe before any beneficial buttressing effect becomes apparent (Fig. 17). Even then, the added benefit of this exceptionally large toe buttress does not act to completely stabilize the slope but only reduces the rate of slope movement.

Fig. 16. Comparison between pore pressures measured at depth in borehole CVM6 and those modelled.

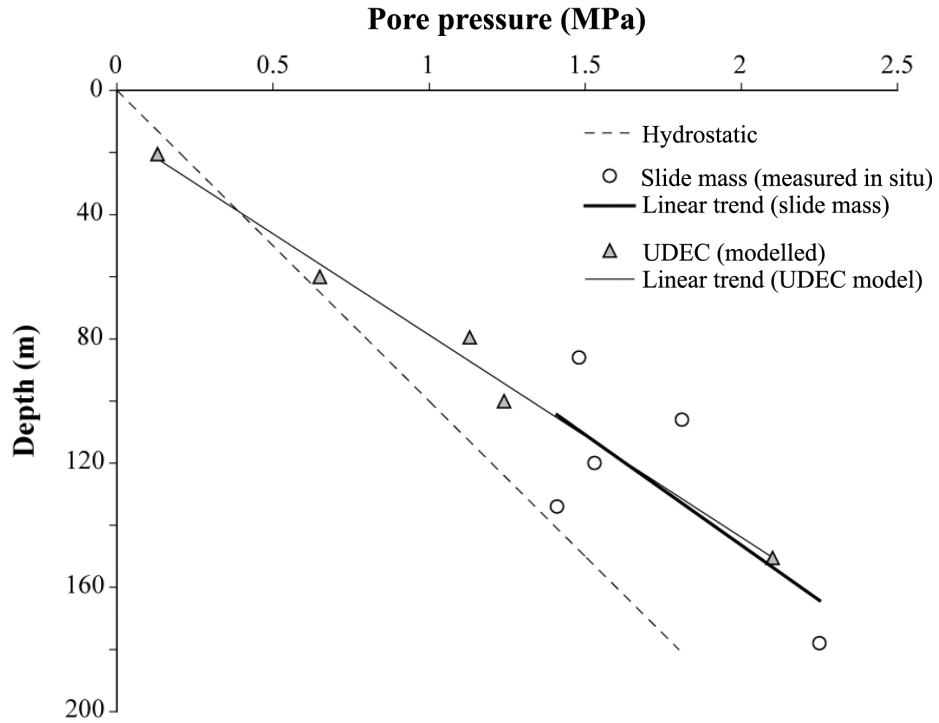


Fig. 17. Comparison of horizontal slope movements assuming the present day situation of an eroded slope toe and those if the past 100 years of erosion of the slope toe were prevented. For comparison, a second hypothetical case is included where the buttressing effect is magnified ten times.

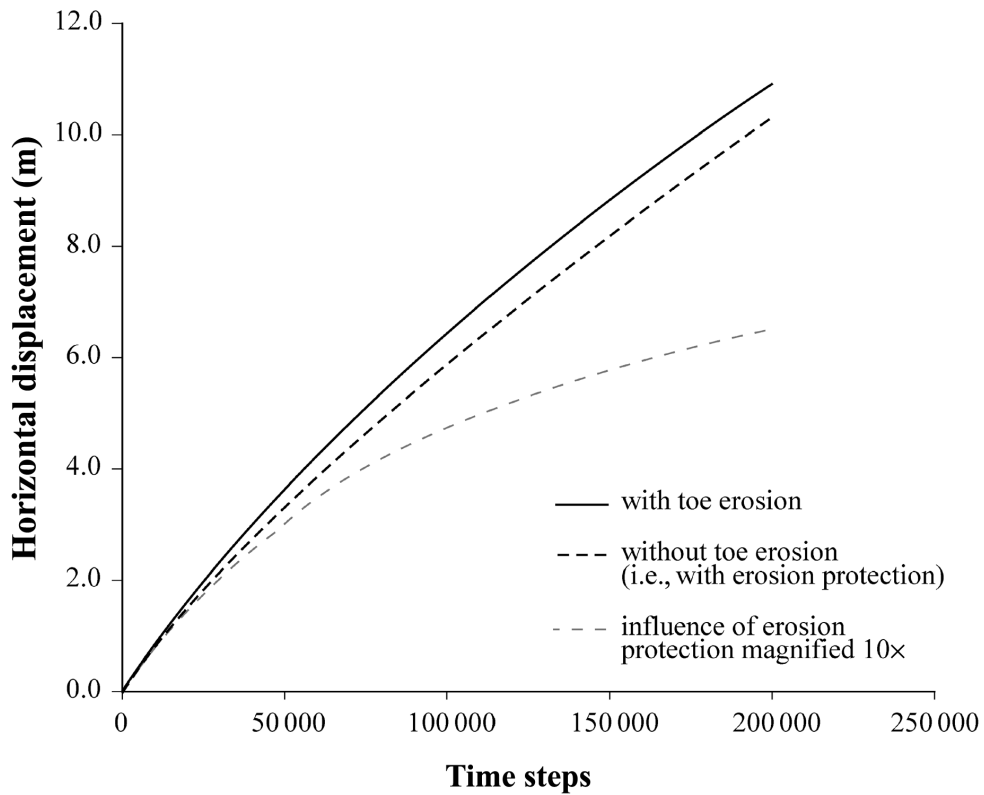


Fig. 18. UDEC modelled pore pressure contours before and after the opening of the drainage adit is simulated in the model.

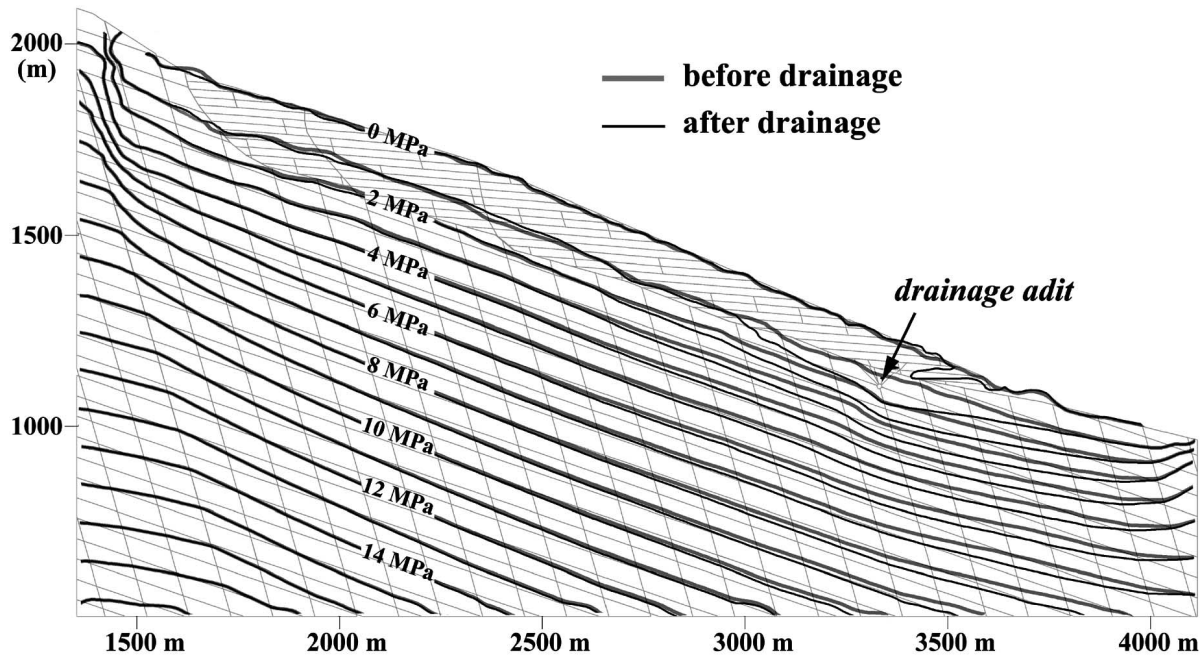
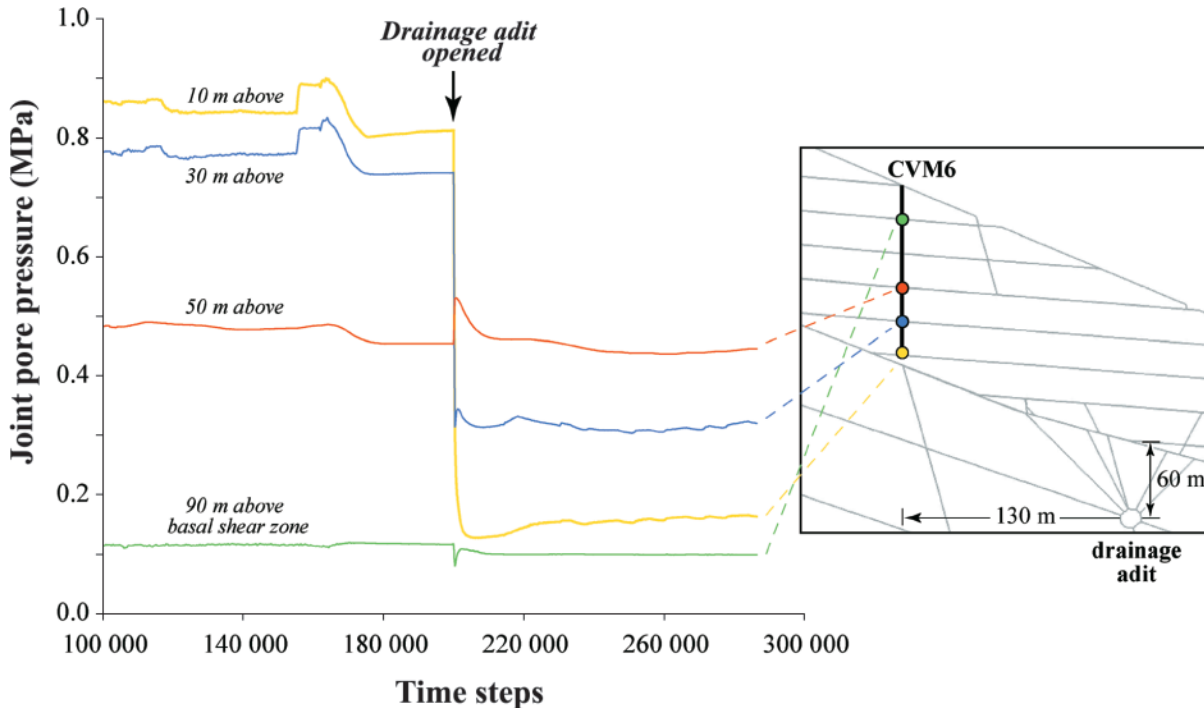


Fig. 19. UDEC modelled pore pressures corresponding to the location of borehole CVM-6. Note the small-scale fluctuations in pore pressures prior to drainage (relating to stick-slip behaviour of unstable slope in the model) and the significant drop in pore pressures at depth after the opening of the drainage adit.

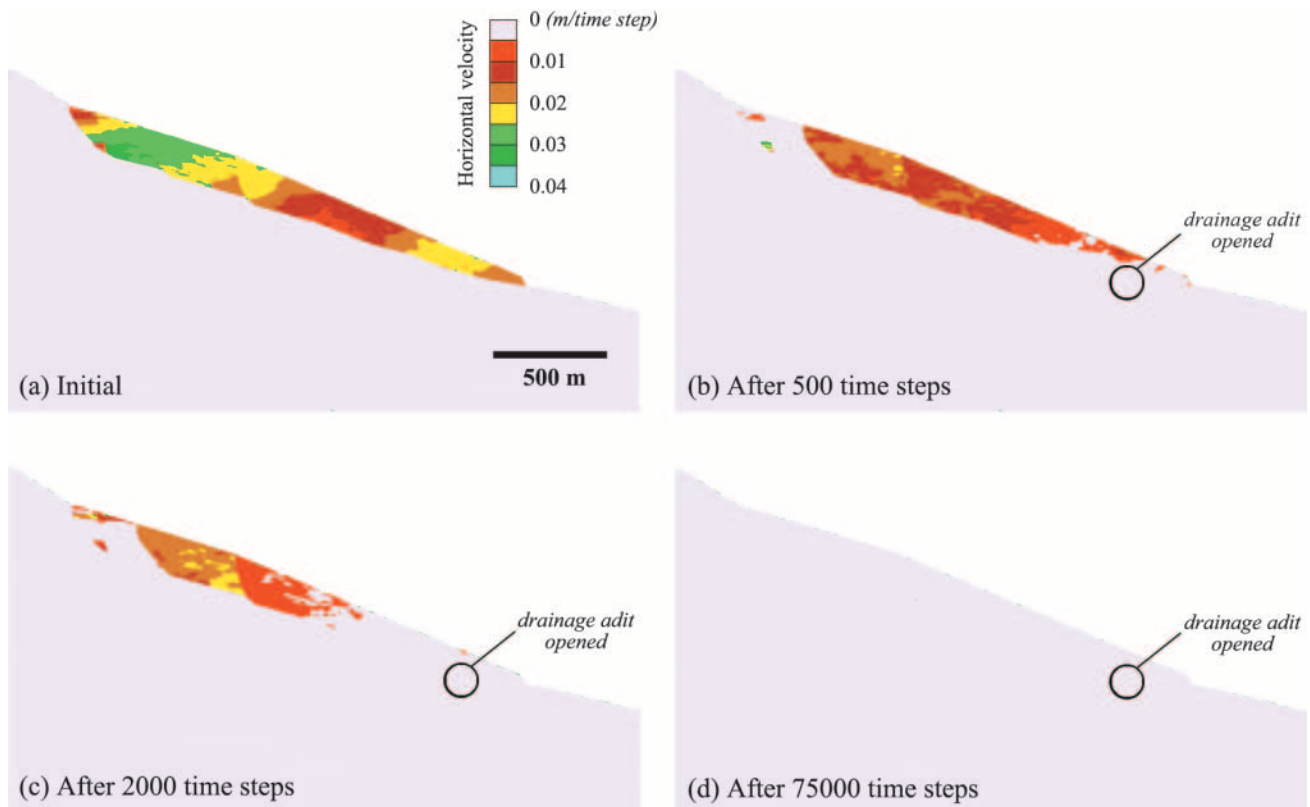


Modelled effects of stabilization through deep drainage

The response of the distinct-element models in which deep drainage was simulated was markedly different; a near immediate stabilization of the slope was produced when the modelled drainage adit was opened. Figure 18 shows the before and after pore pressure contours for the model, with the most noticeable changes occurring below the foot of the landslide. Close to the modelled drainage adit, pore pres-

ures were seen to drop in excess of 1.1 MPa. This agrees reasonably well with corresponding multipoint piezometer values recorded in situ in borehole CVM6. For example, a pore pressure drop of approximately 1.5 MPa (150 m head) was recorded at the lowest piezometer point in borehole CVM6 in response to the opening of the drainage adit (Fig. 8), whereas for the same point in the model, a pore pressure drop of 0.8 MPa was calculated (Fig. 19).

Fig. 20. Modelled horizontal slope velocities *before* and *after* opening of the drainage adit. Note that velocities are not true time-dependent displacement rates (e.g., m/s), but are based on the amount of displacement occurring over each time step.



Concurrent with the modelled drop in pore pressures was a near immediate cessation of horizontal downslope movements in the model. In its unstable state (i.e., prior to drainage), model results show that the slope is unstable along its entire profile with numerical velocities being greatest over the central and lower portions of the landslide (Fig. 20a). Note that these velocities are not true time-dependent displacement rates (e.g., m/s), but are based on the amount of displacement occurring over each time step and thus indicate the degree of instability in the different blocks with higher velocities indicating higher rates of downslope movement. Upon opening of the drainage adit (Fig. 20b), the foot of the landslide immediately begins to stabilize. As the lower slope stabilizes, the passive resistance provided works to stabilize the upper portions of the landslide (Figs. 20c, 20d). A similar response was found even when a more critically unstable slope condition was assumed (i.e., with a frictional strength of 28° along the slide surface). Projecting this into the 3-D case at Campo Vallemaggia, the stabilization of the Campo block would in turn ensure the stabilization of the Cimalmotto block, which it restrains kinematically.

What can also be seen from this model is that the uppermost block at the head of the landslide slips and rotates as space is created in front of it by the moving lower slide blocks. Once the lower blocks decrease their rate of downslope descent, this upper block is one of the first to stabilize (Fig. 20b, 20c).

In terms of water outflows, the model shows that very little drainage is required for this stabilizing effect to occur. For the case shown in Fig. 20, the modelled peak inflow

into the adit was approximately 20 L/s, eventually reaching a steady-state value of 7.5 L/s. This correlates closely with in situ observations made during the drainage works at Campo Vallemaggia, which suggests that the joint pore pressures were significantly reduced even though only a relatively small volume of water flow was captured through the drainage system. The significance of this result is discussed more thoroughly in the next section.

Discussion – Deep drainage in fractured rock masses

The successful use of deep drainage to lower in situ water pressures and stabilize hazardous slopes has been widely documented in a number of case studies (albeit primarily in relation to high porosity soil-colluvium slopes). Those analogous to the Campo Vallemaggia landslide, where deep drainage adit systems have been implemented to stabilize massive, active (or potentially reactivated), deep-seated translational rockslides, are listed in Table 2.

Following the stabilization of Campo Vallemaggia, questions arose as to the effectiveness of the drainage adit (compared to the river diversion and erosion protection works) with some suggesting that outflow rates of 30 L/s were too low to be of any significance given the volume of rock supposedly drained by the 1800 m long adit system. Taking the length of the adit over which drainage occurred, together with half the thickness of the slide mass (i.e., that penetrated by the perforation boreholes) and the minimum and maximum extents of the measured subsidence trough, a drained rock mass volume of 50–75 million cubic metres can be

Table 2. Deep drainage adit systems, analogous to the case of Campo Vallemaggia, implemented to stabilize massive, active or potentially reactivated, deep-seated rockslides along reservoir slopes in connection with major hydroelectric projects.

Dam	Landslide	Slide volume (m ³)	Slide material	Drainage works	Reference
Revelstoke Dam (Canada)	Downie Slide	1500 million	Fractured and faulted mica schists and gneisses	2430 m of tunnel with 13 600 m of drainholes	Imrie et al. (1992); Enegren and Imrie (1996)
Clyde Dam (New Zealand)	Nine Mile Creek (downstream)	>1000 million	Sheared schist and blocky schist debris	4850 m of tunnel with 20 000 m of drainholes	Jennings et al. (1992); Macfarlane and Gillon (1996)
Clyde Dam (New Zealand)	Nine Mile Creek (upstream)	300 million	Sheared schist and blocky schist debris	3300 m of tunnel with 15 000 m of drainholes	Newton and Smith (1992); Jennings et al. (1992)
Clyde Dam (New Zealand)	Brewery Creek Slide	150 million	Sheared mica schist and blocky schist debris	1900 m of tunnel with 12 000 m of drainholes	Gillon et al. (1992b)
Mica Dam (Canada)	Dutchman's Ridge	115 million	Fractured and faulted gneissic and schistose rock	872 m of tunnel with 17 000 m of drainholes	Moore and Imrie (1992)
Clyde Dam (New Zealand)	No. 5 Creek Slide	60 million	Sheared mica schist and blocky schist debris	760 m of tunnel with 6350 m of drainholes	Macfarlane and Jenks (1996)
Tablachaca Dam (Peru)	Tablachaca Dam Landslide	13 million	Fractured phyllite	1527 m of tunnel with 3290 m of drainholes	Millet et al. (1992); Garga and de la Torre (2004)
Clyde Dam (New Zealand)	Cairmuir Landslide	8.3 million	Schist debris and fractured schistose rock	600 m of tunnel with 6000 m of drainholes	Gillon and Saul (1996)
Clyde Dam (New Zealand)	Jackson Creek Landslide	5 million	Schist debris and fractured schistose rock	500 m of tunnel with 7600 m of drainholes	Gillon et al. (1992a)

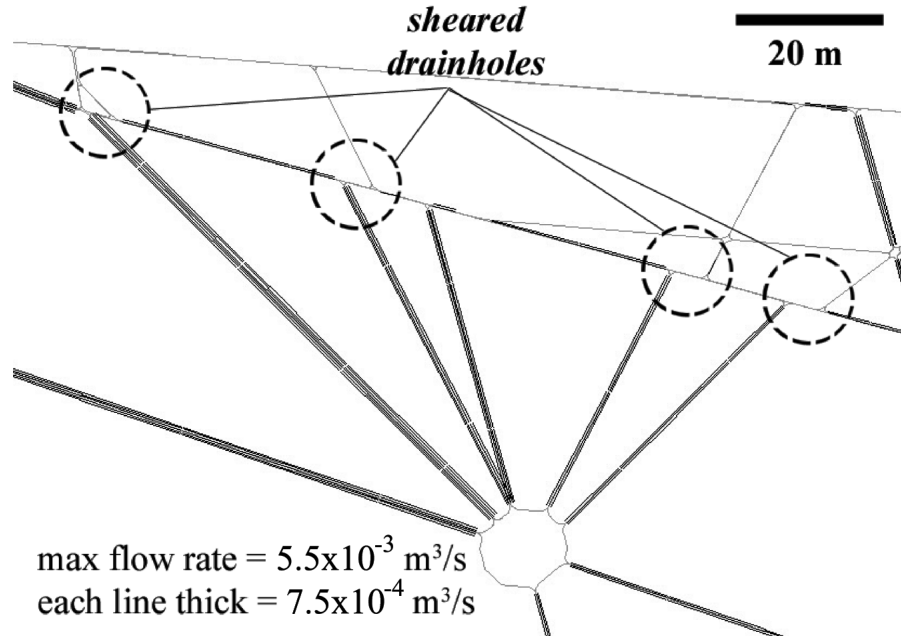
roughly approximated (based on the volume for an inverted pyramidal frustum). From this, drainage outflows ranged from a peak of 50 L/s to an assumed steady state of 10–30 L/s (fluctuating with seasonal variations).

In contrast, Martin and Warren (1992) report outflow rates of 80 L/s during the stabilization of a landslide 1% the size of Campo Vallemaggia, the Taren Landslide in south Wales. The Taren Landslide involved 8 million cubic metres of sandy-silt and broken sandstone slipping on weak mudstone layers. Such comparisons at first make the 30 L/s discharge from the Campo Vallemaggia drainage adit system seem insignificant, especially when comparing the drained volumes involved (approximately 100 times greater in the case of Campo Vallemaggia). However, the Taren Landslide drainage scheme was implemented in fractured sandstone, a much more porous medium than the fractured crystalline rock of Campo Vallemaggia – the key difference being the respective storativities of the two rock masses involved. In the case of Campo Vallemaggia, the flow and drainage problem must be viewed as one involving fracture flow and therefore low storativities. Fracture permeability corresponds to low storativities, therefore large water outflows through drainage are not necessary to achieve significant reductions in head! This was clearly seen in the distinct-element modelling results.

In such cases, the interconnectivity of the fracture permeability system becomes an important consideration with respect to the density of drainage boreholes required to perforate water bearing “compartments” and achieve effective drainage. In several of the cases reported in Table 2 involving deep-seated slides in schists and gneisses, the water tables were described as perched, with permeability barriers dividing the rock mass into isolated compartments (e.g., Dutchman's Ridge, Jackson Creek, Brewery Creek, Nine Mile Creek (upstream); see Table 2 for references). Both Moore and Imrie (1992) and Gillon et al. (1992a) report the use of targeted drilling, thereby ensuring hydraulic connection between major water bearing shear zones and interconnected discontinuity systems. In the case of the drainage of the right abutment of the Tarbela Dam project in Pakistan, situated in carbonaceous and graphitic schist layers, all boreholes were tested to make sure they ended in a pervious zone (Khaliq and Haq 1984).

In terms of outflows, Moore and Imrie (1992) report steady-state flows of 25–50 L/s (depending on seasonal variations) at Dutchman's Ridge, with corresponding drops in head along the basal shear zone of 10 m (50 m in one case). Macfarlane and Jenks (1996) report a drawdown of up to 160 m beneath the No. 5 Creek Slide with outflows of 5 L/s. In the case of the Downie Slide, where the permeability was described as being more homogenous, Imrie et al. (1992) report annual discharges of 35–60 L/s, with some piezometers showing drops in head of over 100 m. These values are very similar to those measured at Campo Vallemaggia. At the Nine Mile Creek (upstream) landslide, Newton and Smith (1992) report the drainage of 710 000 m³ of groundwater over a 21 month period (equivalent to an average outflow of 12.5 L/s), with a drawdown exceeding 200 m in the middle section of the unstable slope. Again, this drainage outflow is comparable to that for Campo, which likewise achieved a similarly impressive drawdown (150 m in head as measured

Fig. 21. UDEC model showing reduced drainage flow in sheared segments of drainholes.



in borehole CVM6). Another shared phenomenon between Nine Mile Creek and Campo Vallemaggia was the measurement of a subsidence trough over the drainage works (>160 mm in the case of Campo, >80 mm after 1 year of drainage in the case of Nine Mile Creek; Jennings et al. 1992). In each of these cases, the significant reductions in head achieved (100–200 m) can be attributed with some certainty to the low storativity and interconnectivity of the fracture flow network. In contrast, the higher outflows (80 L/s) reported by Martin and Warren (1992) generated a lower drawdown of 12–24 m in the more porous sandy-silts and broken sandstones of the Taren Landslide.

The effectiveness of deep drainage in stabilizing the Campo Vallemaggia landslide does not exclude the possibility that the landslide may reactivate in the future. If over time the drainage system breaks down and deteriorates, to the point that the critical sliding zone is no longer being effectively drained, then slope movements may begin again. Imrie et al. (1992) and Macfarlane and Gillon (1996) stress that drainage adits, drainholes, and the instruments monitoring their performance must be regularly inspected and maintained, with drainage boreholes periodically being repaired, reconditioned or re-drilled as their functionality decreases. Enegren and Imrie (1996) provide a detailed overview of the scheduling, rehabilitation, and costs for such a program at the Downie Slide. In reporting the state of the drainage system at the Downie Slide after 10–15 years of use, Imrie et al. (1992) found that a number of drainholes had become plugged or were less efficient. The growth of iron bacteria, borehole collapse, sedimentation, calcification, and shearing of the drainholes along active joints are all problems that may require the drilling of new perforation holes (Imrie et al. 1992; Macfarlane and Gillon 1996). The shearing of drainholes through minor slope movements during drainage and drawdown of pore pressures was likewise found to be an issue in the UDEC simulations (Fig. 21). This may explain why Enegren and Imrie (1996) found little success in

trying to pressure wash and clean less efficient drainholes. In such cases, the only remedy would be to re-drill or replace the drainholes over time, where new drill locations may be required as opposed to reconditioning the existing boreholes. Such considerations are certainly applicable to the drainage works at Campo Vallemaggia, and as such, pressure must be maintained on the responsible authorities to budget for maintenance work appropriately.

Conclusions

Stabilization of the deep-seated Campo Vallemaggia landslide in southern Switzerland was carried out implementing two mitigation strategies – erosion protection of the slope's toe through the diversion of the river undercutting it and deep drainage through the construction of a drainage adit from which drainage boreholes were drilled into the base of the unstable landslide. These measures were not designed to complement one another, but were the byproduct of competing expert opinions as to what the underlying mechanisms controlling the instability were.

Results from a detailed investigation (presented in Part I, Bonzanigo et al. 2007) showed that the deep-seated landslide involved approximately 800 million cubic metres of metamorphic crystalline rock, reaching depths of approximately 300 m, divided into a complex assemblage of blocks by tectonic faults and internal shearing. These movements eventually led to a critical situation that threatened the destruction of two villages, Campo Vallemaggia and Cimalmotto, located on the lower sections of the unstable slope.

Numerical modelling results, based on hydromechanically coupled distinct-element models, strongly suggest that deep drainage was the key measure that brought about the successful stabilization of the landslide. Modelling results accounting for erosion protection measures at the toe of the landslide showed that the extra buttressing effect afforded by the noneroded material was insignificant given the driv-

ing mass of the unstable slide body. On the contrary, the simulation of deep drainage in the model (constrained by in situ piezometer measurements) showed a near immediate stabilization of the slope with very little drainage outflow required. These results agree with in situ observations of outflows following the construction of the drainage adit. Although these same low outflows contributed towards scepticism as to the effectiveness of the deep drainage mitigation solution, the modelling results clearly show that in the case of fracture permeability, where the storativities are low, large water outflows through drainage are not necessary to achieve significant reductions in head.

It is still not clear yet whether steady-state conditions have been reached in the drainage adit. If not, then they are expected in the next few years. Regular inspections of the drainage works should be implemented to ensure that blockages to the system do not occur or to bring attention to any declines in the system's effectiveness that may call for reconditioning and (or) redrilling of the drainholes.

Acknowledgements

The authors would like to thank Prof. Conrad Schindler and Dr. Giovanni Lombardi for their contributions in the early days of this work. The authors also wish to acknowledge Fulvio Caccia and Renzo Respini, former ministers for the environment, for the political support they provided, and Pierfrancesco Bertola of Lombardi Ltd. for the efficient and challenging design of the adit. Thanks are also extended to Marco Broglio and "sindaco" (Maire), of Campo Vallemaggia, together with the other inhabitants living in the investigation area who allowed access to their properties for the field investigation and borehole drilling campaigns. Partial funding in support of this work has been made available through a Natural Sciences and Engineering Research Council of Canada (NSERC) Discovery grant.

References

- Bonzanigo, L. 1999. Lo slittamento di Campo Vallemaggia. D.Sc. thesis, Engineering Geology, Swiss Federal Institute of Technology (ETH Zurich), Zurich, Switzerland.
- Bonzanigo, L., Eberhardt, E., and Loew, S. 2007. Long-term investigation of a deep-seated creeping landslide in crystalline rock. Part I. Geological and hydromechanical factors controlling the Campo Vallemaggia landslide. *Canadian Geotechnical Journal*, **44**: 1157–1180.
- Engren, E.G., and Imrie, A.S. 1996. Ongoing requirements for monitoring and maintaining a large remediated rockslide. *In Proceedings of the 7th International Symposium on Landslides, Trondheim. Edited by K. Senneset. A.A. Balkema, Rotterdam. Vol. 3. pp. 1677–1682.*
- Garga, V.K., and de la Torre, M. 2004. The Tablachaca Slide No. 5, Peru – a 20-year post-remediation assessment. *In Proceedings of the 9th International Symposium on Landslides, Rio de Janeiro. Edited by W.A. Lacerda et al. A.A. Balkema, Leiden. Vol. 2. pp. 1691–1696.*
- Gillon, M.D., and Saul, G.J. 1996. Stabilisation of Cairnmuir Landslide. *In Proceedings of the 7th International Symposium on Landslides, Trondheim. Edited by K. Senneset. A.A. Balkema, Rotterdam. Vol. 3. pp. 1693–1698.*
- Gillon, M.D., Anderson, C.K., Halliday, G.S., and Watts, C.R. 1992a. Jackson Creek landslide stabilisation, New Zealand. *In Proceedings of the 6th International Symposium on Landslides, Christchurch. Edited by D.H. Bell. A.A. Balkema, Rotterdam. Vol. 1. pp. 707–713.*
- Gillon, M.D., Graham, C.J., and Grocott, G.G. 1992b. Low level drainage works at the Brewery Creek Slide. *In Proceedings of the 6th International Symposium on Landslides, Christchurch. Edited by D.H. Bell. A.A. Balkema, Rotterdam. Vol. 1. pp. 715–720.*
- Heim, A. 1897. I movimenti di terreno di Campo V.M. *Report by Albert Heim (translated from German into Italian by Alberto Totanzi, Cimalmotto).*
- Heim, A. 1932. *Bergsturz und Menschenleben.* Fretz and Wasmuth Verlag, Zurich. p. 218.
- Imrie, A.S., Moore, D.P., and Energen, E.G. 1992. Performance and maintenance of the drainage system at Downie Slide. *In Proceedings of the 6th International Symposium on Landslides, Christchurch. Edited by D.H. Bell. A.A. Balkema, Rotterdam. Vol. 1. pp. 751–757.*
- Itasca. 2004. UDEC - Universal Distinct Element Code, Version 4.0 [computer program]. Itasca Consulting Group, Inc., Minneapolis, Minn.
- Jennings, D.N., Newton, C.J., Beetham, R.D., and Smith, G. 1992. Stabilization of the Nine Mile Creek schist landslide complex. *In Proceedings of the 6th International Symposium on Landslides, Christchurch. Edited by D.H. Bell. A.A. Balkema, Rotterdam. Vol. 1. pp. 759–764.*
- Khaliq, A., and Haq, I. 1984. Rock slide right abutment hill – Tarbela. *In Proceedings of the 4th International Symposium on Landslides, Toronto. University of Toronto Press, Downsfield. pp. 529–534.*
- Lichtenhahn, C. 1971. Zwei Stollenbauten: Stollen im Eis zur Verhinderung von Ausbrüchen eines Sees im Grubengletschergebiet (Wallis) und Stollen im Felsen zur unterirdischen Entwässerung des Rutschgebietes von Campo Vallemaggia (Tessin). *Interprevent*, **344**: 465–476.
- Lombardi, G. 1996. Der Drainagestollen von Campo, Rovana. *Wasser, Energie, Luft*. **88**: 281–287.
- Macfarlane, D.F., and Gillon, M.D. 1996. The performance of landslide stabilisation measures, Clyde Power Project, New Zealand. *In Proceedings of the 7th International Symposium on Landslides, Trondheim. Edited by K. Senneset. A.A. Balkema, Rotterdam. Vol. 3. pp. 1747–1757.*
- Macfarlane, D.F., and Jenks, D.G. 1996. Stabilisation and performance of No. 5 Creek slide, Clyde Power Project, New Zealand. *In Proceedings of the 7th International Symposium on Landslides, Trondheim. Edited by K. Senneset. A.A. Balkema, Rotterdam. Vol. 3. pp. 1739–1746.*
- Martin, P.L., and Warren, C.D. 1992. The design and performance of drainage measures installed for the stabilisation of Taren Landslide, South Wales, UK. *In Proceedings of the 6th International Symposium on Landslides, Christchurch. Edited by D.H. Bell. A.A. Balkema, Rotterdam. Vol. 1. pp. 777–784.*
- Millet, R.A., Lawton, G.M., Repetto, P.C., and Garga, V.K. 1992. Stabilization of Tablachaca Dam Landslide. *In Proceedings, Stability and Performance of Slopes and Embankments – II, Berkeley. Edited by R.B. Seed and R.W. Boulanger. Geotechnical Special Publication No. 31, American Society of Civil Engineers, N.Y. pp. 1365–1381.*
- Moore, D.P., and Imrie, A.S. 1992. Stabilization of Dutchman's Ridge. *In Proceedings of the 6th International Symposium on Landslides, Christchurch. Edited by D.H. Bell. A.A. Balkema, Rotterdam. Vol. 3. pp. 1783–1788.*
- Newton, C.J., and Smith, G. 1992. Dewatering of the Nine Mile Creek Landslide. *In Proceedings of the 6th International Symposium on Landslides, Christchurch. Edited by D.H. Bell. A.A. Balkema, Rotterdam. Vol. 1. pp. 797–803.*

- Priest, S.D. 1993. Discontinuity analysis for rock engineering. Chapman & Hall, London. p. 473.
- Stead, D., Eberhardt, E., and Coggan, J.S. 2006. Developments in the characterization of complex rock slope deformation and failure using numerical modelling techniques. *Engineering Geology*, **83**: 217–235. doi:10.1016/j.enggeo.2005.06.033.
- Terzaghi, K. 1950. Mechanism of landslides. *In* Application of geology to engineering practice. *Edited by* S. Paige. *Engineering Geology* (Berkey) Volume, The Geological Society of America, New York. pp. 83–123.
- Terzaghi, K., and Peck, R.B. 1967. Soil mechanics in engineering practice. 2nd ed. John Wiley & Sons, New York. p. 729.